論 文
33〜4〜5

실리콘 結晶의 方向性에 따른 Turn-On 電圧과 表面狀態密度의 依存性에 관한 研究

Dependence of Turn-On Voltage and Surface State Density on the Silicon Crystallographic Orientation

成 英 權* · 成 萬 永** · 趙 哲 済*** · 高 基 萬**** · 李 炳 得*****
(Young-Kwon Sung · Man-Young Sung · Cheol-Jee Cho · Gi-Man Ko · Beong-Deug Lee)

요 약

本 論文은 이온농도 측정을 위한 GCD (Gate Controlled Diode)의 試作에 관한 研究의 一部分으로서 Si 結晶의 方向性 즉 (100)과 (111)에 대한 turn on 電壓과 表面狀態密度의 영향에 관하여 考察하였다. 따라서 各 測定條件에 따라 (100) 및 (111) 面으로 製作된 試料素子에 대하여 turn on 電壓과 表面狀態密度의 영향에 관하여 관찰하였으며 turn-on 電壓에 의하여 決定되는 interfacial trap 에 있어서의 增加는 表面生成-再結合 速度의 增加에 직접적으로 비례한다는 것을 알 수 있었다.

Abstract

The object of this paper is to investigate the gate controlled diode structure for ionic concentration. measurement. It includes device fabrication, characterization, device physics and modeling of the gate controlled diode structure. The differences of turn on voltages and surface generation currents in the (100) and (111) silicon crystallographic orientation of the sample device were observed. Therefore the dependence of these two factors on the silicon crystallographic orientation was investigated. It was observed that drifts arose after extended immersion of the sample device in acid or base solutions. The surface generation-recombination velocity of both (100) and (111) increased. The increase in the interfacial traps for both surface, determined by the turn on voltage was directly proportional to the surface generation-recombination velocity increase.

I. Introduction

It has been long known that the surface state density at the Si-SiO_2 interface for a given set of oxidation conditions is larger on (1 1 1) oriented surface than on (1 0 0) surfaces.[1),2)] It is also well known that the fixed oxide charge located within 100Å of the insulator-semiconductor interface depends on the oxidation, annealing conditions and, on occasion, the crystallographic orientation of the surface.[3),4)]

While these effects can be demonstrated in a number of ways, one of the simplest is the MOS C-V method.[5),6)] As far as we can determine, all of these studies employed different silicon substrate samples for the different crystallographic orientations. Under these conditions, it is difficult to assure that the specimens were subject to identical processing. For the sample device in Fig. 1, we investigated the effect of surface conditions on a device that contained both the (1 0 0) and (1 1 1) crystallographic orientations. Since the device contained both surface in its active region, they can

* 正 会 員：高麗大 工大 電気工学科 教授・工博
** 正 会 員：檀国大 工大 電気工学科 教授・工博
*** 正 会 員：高麗大 大学院 電気工学科 博士課程
**** 正 会 員：檀国大 大学院 電気工学科 碩士課程
***** 正 会 員：高麗大 大学院 電気工学科 碩士課程
接受日字：1983年12月21日

be processed and measured under exactly the same conditions.

The C-V characteristics of the junction are compared to the p-n junction reverse bias current at corresponding values of the reference electrode bias, V_g. The values for the turn on voltage for the two crystallographic faces are obtained from this data. The effect of oxide charges and surface states on the surface generation current is examined. We consider the role of the lattice geometry at the Si-SiO_2 interface on the chemical activity of the two crystallographic faces.

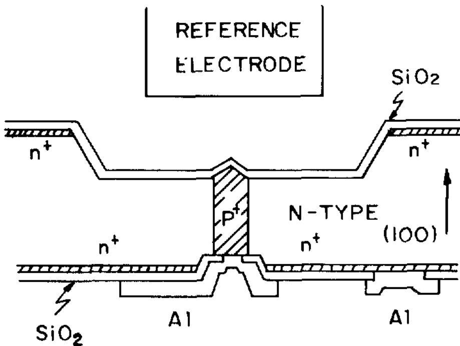

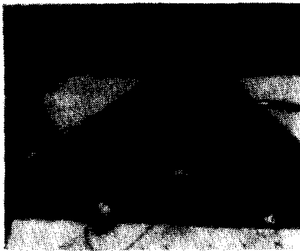

Fig. 1. Structure of the sample device for the investigation.

II. Basic Theory

The threshold voltage for a MOS capacitor structure is[7]

$$V_T = V_{To} + \frac{Q_{ox} + Q_{ss}}{C_{ox}} \tag{1}$$

where V_{To} is the ideal thershold voltage

$$V_{To} = -\frac{Q_B}{C_{ox}} + 2\,\phi_{FB} + V_J + \phi_{sol,S} \tag{2}$$

Q_B is the bulk charge density in a screening length, C_{ox} is the oxide capacitance, ϕ_{FB} is the bulk Fermi level, V_J is the substrate-channel junction voltage and $\phi_{sol,\ S}$ is the solution-silicon work function difference. We ignore the reference electrode-solution interphase potential though it should be included in $\phi_{sol,S}$. There is no information available to our knowledge on $\phi_{sol,S}$.

As noted in reference 7, V_T is a function of the crystallographic face of the device. V_{To} is independent of face (assuming that this indenpendence is valid for $\phi_{sol,S}$). We also make an important assumption that the oxide charge, Q_{ox}, is a function of the preparation conditions but not of crystal face. There is recent evidence to support this assumption based on the work of Kasprzak, Gaind on deposited CVD oxides.[8] The fast surface charge density is Q_{ss} and it will depend on crystallographic orientation, i.e. $Q_{ss}^{(111)}$ and $Q_{ss}^{(100)}$. We use the subscript notation 0, 1 to refer to initial and final values for the threshold voltages, $V_{T,O}^{(111)}$, $V_{T,1}^{(111)}$, $V_{T,0}^{(100)}$ and $V_{T,1}^{(100)}$. This gives us a set of equations

$$V_{T,0}^{(111)} = V_{To} + \frac{Q_{ox,0}}{C_{ox}} + \frac{Q_{ss,0}^{(111)}}{C_{ox}}\ ;$$

$$V_{T,0}^{(100)} = V_{To} + \frac{Q_{ox,0}}{C_{ox}} + \frac{Q_{ss,0}^{(100)}}{C_{ox}} \tag{3}$$

$$V_{T,1}^{(111)} = V_{To} + \frac{Q_{ox,1}}{C_{ox}} + \frac{Q_{ss,1}^{(111)}}{C_{ox}}\ ;$$

$$V_{T,1}^{(111)} = V_{To} + \frac{Q_{ox,1}}{C_{ox}} + \frac{Q_{ss,1}^{(100)}}{C_{ox}} \tag{4}$$

The peak current for the reverse bias substrate channel current I_R is assumed to be due to a density of surface recombination centers, N_R. This density in turn, is assumed to be proportional to the fast state density Q_{ss}. Thus

$$\left.\begin{aligned} I_{R,0}^{(111)} &= \alpha A^{(111)}\, Q_{ss,0}^{(111)}/C_{ox} \\ I_{R,1}^{(111)} &= \alpha A^{(111)}\, Q_{ss,1}^{(111)}/C_{ox} \end{aligned}\right\} \tag{5}$$

$$\left\{\begin{array}{l} I_{R,0}^{(100)} = \alpha A^{(100)} Q_{ss,o}^{(100)}/C_{ox} \\ I_{R,1}^{(100)} = \alpha A^{(100)} Q_{ss,1}^{(100)}/C_{ox} \end{array}\right\} \quad (6)$$

where α is a proportionality constant. By combining these equations we obtain the important consistency relation.

$$\alpha = \frac{\left\{\dfrac{I_{R,1}^{(111)}}{A^{(111)}} - \dfrac{I_{R,1}^{(100)}}{A^{(100)}}\right\}}{V_{T,1}^{(111)} - V_{T,1}^{(100)}} = \frac{\left\{\dfrac{I_{R,0}^{(111)}}{A^{(111)}} - \dfrac{I_{R,0}^{(100)}}{A^{(100)}}\right\}}{V_{T,0}^{(111)} - V_{T,0}^{(100)}} \quad (7)$$

III. Experimental Results

1) C/V_g characteristics

The sample device was immersed in a 0.1M KCl solution for test and the gate bias was applied through a silver/silver chlolide reference electrode. The admittance of the P-N junction was measured at a frequency of 10 KHz. The C/V_g characteristics were obtained for P-N junction biases ranging from 0.0 volt to −1.0 volt as shown in Fig. 2. When V_g was sufficiently negative, the surface was driven into inversion and the measured capacitance rose. This value saturated at the depletion layer capacitance when the sample device was heavily inverted and was dependent on the P-N junction bias. When P-N junction was reverse biased, the depletion region widened, requiring a higher electric field at the silicon surface to invert the surface. In other words, the higher negative bias needed to turn on the inversion layer shifted the curves to a more negative gate bias as the P-N junction reverse bias increased. The saturated capacitance value was also reduced due to the widening of the depletion layer. The pronounced kink occuring in the mid range of the capacitance for each curve is due to the different turn on voltages of the (100) and (111) interfaces which arises from the different surface state densities at these interfaces.

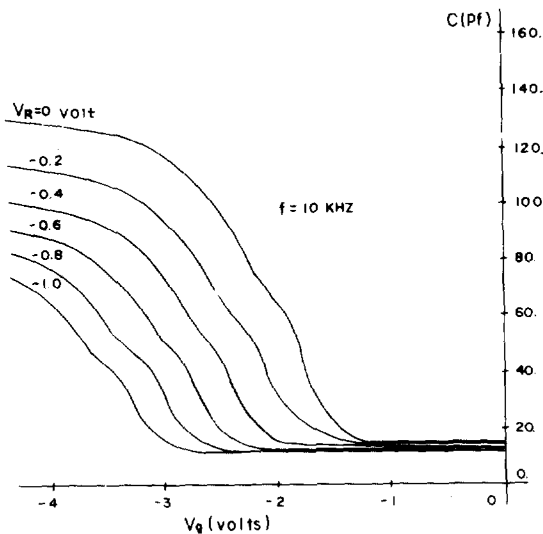

Fig. 2. C/V_g characteristics with P-N junction bias as a parameter.

2) I_R/V_g characteristics

The current flowing through the P-N junction was measured with respect to the gate bias voltage at fixed P-N junction reverse bias. The $I_R(V_g, V_R)$ characteristics with the reverse bias as a parameter are shown in Fig. 3. When the surface under the gate is accumulated only those currents due to the metallurgical junction contribute to the reverse bias current. When the surface is operated in depletion, the generation current in this depletion layer will increase as its width is widened. Once the surface is depleted, the generation-recombination

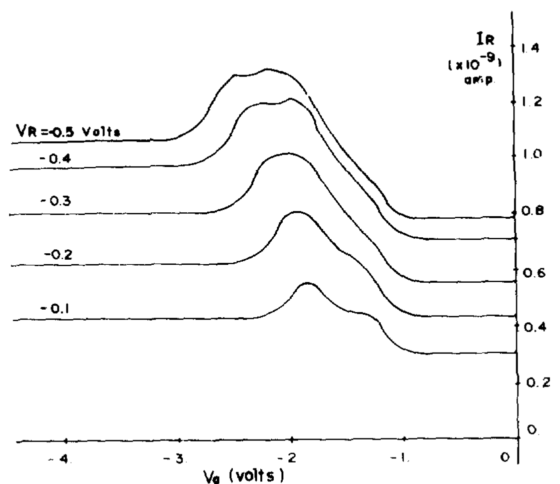

Fig. 3. I_R/V_g characteristics with P-N junction bias as a parameter.

centers at the oxide-silicon interface provide another contribution to the total current. This contribution produces a peak in the $I_R(V_g, V_R)$ characteristics due to the surface potential dependence of the surface recombination rate.
When the surface is driven into inversion, the current decreases, although not to its original value, since the surface generation-recombination centers are screened by the inversion layer. In Fig. 3, we see the structure caused by the different turn-on voltage for (1 0 0) and (1 1 1) interfaces.

It is interesting to compare this $I_R(V_g, V_R)$ curves with the corresponding $C(V_g, V_R)$ curves at fixed V_R. For example, at V_R=−0.4 V, when V_g<−1.4V, the surface is in accumulation so that both the capacitance and reverse current have a constant value. As V_g approaches −1.0V, the (1 0 0) surface starts to deplete resulting in the an increased reverse generation current. However weak depletion does not influence the capacitance. When V_g is near −1.3V, the (1 1 1) surface begins to deplete. The generation current due to this (1 1 1) depletion layer and to miscellaneous surface states adds on to the original (1 0 0) generation current causing a pronounced kink in the curve. When V_g rises to −1.95V, the (1 0 0) surface is driven into inversion and the reverse current decreases due to the decrease of the surface generation-recombination velocity on (1 0 0) surface. Meanwhile, this is the point where the capacitance starts to increase because of the formation of the P inversion layer junction area. Note that the decrease of observed current is relatively small. Although the reverse diode current from the surface recombination centers are contributed by both (1 0 0) and (1 1 1) surfaces, we can see that the surface state generation current from (1 0 0) is smaller. More rigorously we should say the surface states with energy levels within a few kT of center mid gap is small, since only the surface states within this energy range are effective as generation-recombination centers. By further decreasing V_g to about −2.25 V, the depletion layer of (1 1 1) surface commences to invert resulting in a further decrease of the P-N junction current. This decrease is larger than the comparable decrease for the (1 0 0) surface, indicating that the density of surface states for the (1 1 1) surface (with energy near mid gap) is larger than that for the (1 0 0) surface. Also there is an approximately 0.3V difference in the turn on voltage for these two surfaces. Since the loss term arising from the finite resistivity of the inversion layer influences the capacitance measurement at 10KHz, the pronounced (1 1 1) capacitance contribution can only be observed when V_g is less than −2.75V.

The depletion layer generation current and surface generation current are related to the generation-recombination time constant τ_o and surface generation-recombination velocity S_o respectively by the following formula.[7]

$$I_{gs} = \frac{1}{2} q n_i S_O A_s \tag{8}$$

$$I_{gd} = \frac{1}{2} q n_i X_{dmax} A_s / \tau_o \tag{9}$$

Where n_i is the intrinsic carrier concentration, A_s the total junction area and X_{dmax} the maximum depletion width. From the data in Fig. 3, τ_o can be estimated to be approximately 2μs, while S_o for the (1 0 0) surface is estimated to be of the order of 10cm/sec and 100cm/sec for the (1 1 1) surface.

The generation-recombination time constant and the surface generation-recombination velocity can also be related to the surface state density via $\tau_o=1/(\sigma_t.V_{th}.N_t)$ and $S_o=\sigma_{st}.V_{th}.N_{st}$. Here N_t is the concentration of bulk generation-recombination centers, σ_t, σ_{st} the capture cross section, V_{th} the thermal velocity of the electrons and N_{st} the density of the surface genertion-recombination centers. If we put in such reasonable values as $\sigma_{st}\sim\sigma_t\sim10^{-16}$ cm^2 and V_{th} = 10^7 cm/sec,[9] we can estimate $N_t\sim5x10^{14}$ cm^{-3} and $N_{st}\sim10^{11}$ cm^{-2} for the (1 1 1) surface and about 10^{10} cm^{-2} for (1 0 0) surface. It can be seen that the surface state density for the (1 1 1) surface is about one order of magnitude higher than that for (1 0 0) surface. In the above case, since the turn on voltage difference is not particularly large, the effects of (1 0 0) and

(1 1 1) surfaces are mixed together in the C/V_g and I_R/V_g measurements. If it is possible to have a larger turn on voltage difference between these two surfaces, then it might be easier to differentiate each effect individually.

After continuous immersion in an aqueous solution for over three weeks, we observed a substantial negative shift of the turn on voltage for the (111) interface region but no shift for the (100) interface. A comparison of the $C(V_g, V_R=0)$ characteristics of an as prepared diode (curve A) and the same structure after aging C (curve B) are shown in Fig. 4. During storage under dry ambient air conditions for two months, we observed a steady but slow drift of both the (100) and (111) interface turn on voltages. This is curve C in Fig. 4. $I_R(V_g, V_R=0.05)$ measurements were obtained as well as the $C(V_g, 0)$. After the aging process, the two barely resolved peaks at the (100) and (111) turn on voltage (difference of 0.3 volts) are now well resolved and are separated by 2 volts (Fig. 5). The increased base level of the reverse current appears to arise from surface leakage at the back contact rather than from recombination processes.

IV. Discussion

As noted in section 2, using the values in Table 1 obtained from Fig.6(a), (b) for sample 1, We find that

$$\frac{1.6\times 10^{-10}}{A(111)}\leq\alpha\leq\frac{2.3\times 10^{-10}}{A(111)} \tag{10}$$

The spread in values is of the order of ±20%, values that are acceptable in view of the uncertainties in both our measurements and assumptions. Proceeding with this value, we obtain the parameters

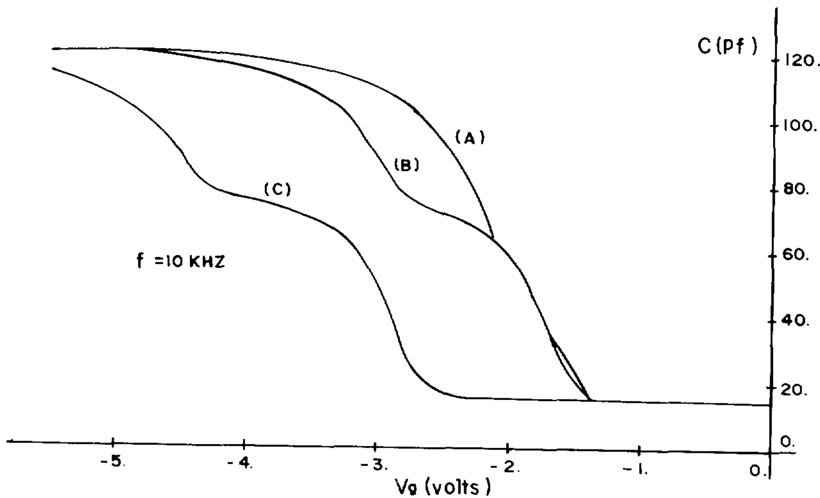

Fig. 4. C/V_g characteristics before (A) and after degradation (B and C).

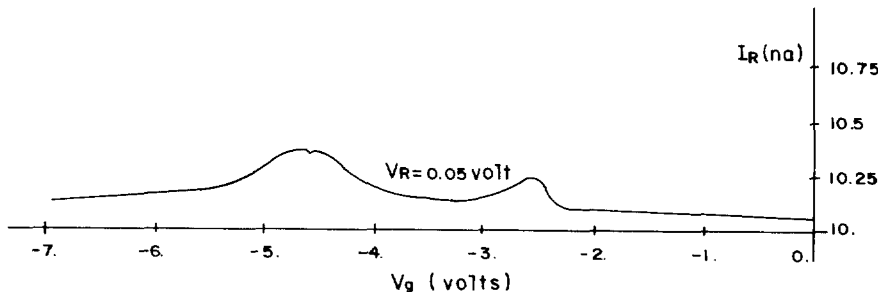

Fig. 5. I_R/V_g characteristics after degradation.

Table 1. Measured turn-on voltage and P-N junction current before and after degradation for both (1 0 0) and (1 1 1) faces.

	Volts		Amperes
$V_{T,0}^{(100)}$	−1.35	$I_{R,0}^{(100)}$	$2.\ x10^{-11}$
$V_{T,1}^{(100)}$	−1.76	$I_{R,1}^{(100)}$	$6.5x10^{-11}$
$V_{T,0}^{(111)}$	−1.83	$I_{R,0}^{(111)}$	$1.2x10^{-10}$
$V_{T,1}^{(111)}$	−2.92	$I_{R,1}^{(111)}$	$2.15x10^{-10}$

$A^{(100)}/A^{(111)} = 1.86$

listed in Table 2 for the surface state densities, oxide charge and, $\phi_{sol,S}$. The values for Q_{ss} are quite respectable given the preparation conditions. The value of $Q_{ss,0}^{(111)}$ and $Q_{ss,0}^{(100)}$ within the range quoted by IC manufacturers.

The most interesting result, then, is the substantial change in surface states $\Delta Q_{ss}^{(111)}$, compared to $\Delta Q_{ss}^{(100)}$, i.e. $1.3x10^{11}/cm^2$ for (1 1 1) compared to $3.4x10^{10}/cm^2$ for (1 0 0). This confirms the change illustrated in Fig.6(a) and (b) in a more quantitative fashion.

Whatever is the source of these interfacial states, it is clear that it involves a reaction at the oxide-solution interface and subsequent transport of an electronically active species to the $Si\text{-}SiO_2$ interface where it preferentially reacts with (1 1 1) surface. One example of preferential reactions is the etching of the Si surface by KOH-Isopropyl alcohol (IPA). This phenomena illustrates the fact that these two surfaces are quite distinct chemically. The preferential etching by the KOH-IPA solution occurs at the silicon-etchant interface. What we find surprising is that a marked chemical difference appears to persists in our samples under a 1500 Å oxide.

It may be worthwhile to use an analogy between observations on the KOH-IPA differential etching

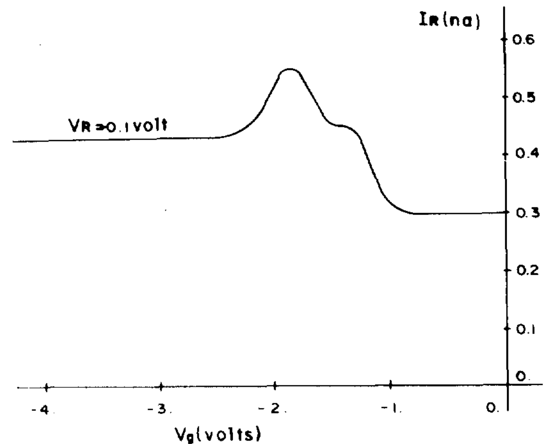

(a)

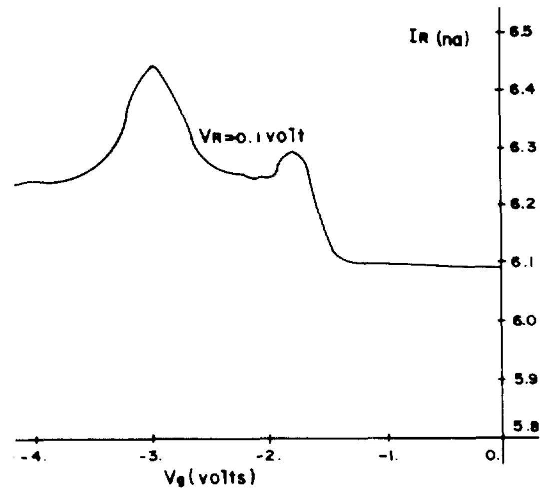

(b)

Fig. 6. I_R/V_g characteristics before degradation (a) and after degradation (b).

Table 2. Calculated surface state density and oxide charge plus ideal turn-on voltage V_{To} for both (100) and (111) faces.

	cm^{-2}		cm^{-2}		Volts
$Q_{ss,0}^{(111)}$	$1.66x10^{11}$	$Q_{ss,0}^{(100)}$	$9.7x10^{10}$	$V_{To} + \frac{Q_{ox,0}}{C_{ox}}$	−0.677
$Q_{ss,1}^{(111)}$	$2.97x10^{11}$	$Q_{ss,1}^{(100)}$	$1.3x10^{11}$		
$\Delta Q_{ss}^{(111)}$	$1.3\ x10^{11}$	$\Delta Q_{ss}^{(100)}$	$3.3x10^{10}$	$V_{To} + \frac{Q_{ox,1}}{C_{ox}}$	−0.854

and the conclusions obtained by Kazprzak and Gaind[8] that atomic hydrogen chemisorbs preferentially on the (1 1 1) surface, then relatively long chain alcohols like IPA may also preferentially bind to the (1 1 1) surface. As a result, we may speculate that there is a correlation between the differential etching of silicon and the incidence of interfacial states on the various crystallographic faces. Studies of the effect of IPA adsorption on (1 1 1) and (1 0 0) surfaces would be interesting.

Unpublished work at this research room indicates that atomic hydrogen can produce a trapping state at the Si-SiO_2 interface. This supports the general conclusion of Kazprzak and Gaind since these measurements were conducted on (1 1 1) surfaces. However, there is no information as yet on (1 0 0) surfaces. The role of H at the Si-SiO_2 interface still remains quite speculative but the weight of evidence is growing on its importance. Experimental tests of this speculation may provide insight not only on etching and degradation process, it may also assist in explaining the behavior of Pd based MIS structures currently being studied as H_2 sensors.

V. Conclusions

The experiments described provide an insight into the chemistry of the (1 1 1) and (1 0 0) Si-SiO_2 interfaces. The fact that continued immersion in acid/base solutions and application of inversion layer fields produces changes in the surface state densities under 1500 Å of oxide suggests that there is either substantial drift of charged species from the solution-oxide interface to the Si-SiO_2 interface or the formation of a neutral species at the solution oxide interface and a diffusion of these neutral species to the Si-SiO_2 interface. The possible relation to selective etching is attractive. We suggest that chemisorptive processes are involved in our measurements as in the etching and H_2 detection processes.

Reference

1) P.V. Gray and D.M. Brown, "Density of SiO_2-Si interface states", Appl. Phys. Letters, Vol. 8, 31-33, 1966.
2) D.R. Frankl, "Comment on Density of SiO_2-Si Interface States by Gray and Brown", J. Appl. Phys., Vol. 38, 1996, 1967.
3) B.E. Deal, M. Sklar, A.S. Grove and E.H. Snow, "Characteristics of the Surface Charge of Thermally Oxidized Silicon", J. Electrochem. Soc., Vol. 114, 266-274, 1967.
4) B.E. Deal, "The Current Understanding of Charges in the Thermally Oxidized Silicon Structure", J. Electrochem. Soc., Vol. 121, 198c-205c, 1974.
5) E.H. Nicollian and A. Goetzberger, "MOS Conductance Technique for Measuring Surface State Parameters", Appl. Phys. Letters, Vol. 7, 216-219, 1965.
6) E.H. Nicollian and Goetzberger, "The SiO-SiO_2 Interface-Electrical Properties as Determined by the Metal-Insulator-Silicon Conductance Technique", Bell Syste. Tech. J., Vol. 46, 1055-1061, 1967.
7) S.M. Sze, Physics of Semiconductor Device, John Wiley (N.Y.), 1968.
8) L.A. Kasprzak and A.K. Gaind, Proc. International Topical Conference, 438 , 1978.
9) A.S. Grove, Physics and Technology of Semiconductor Devices, John Wiley (N.Y.), 1967.